

Article

Interconnections between Coastal Sediments, Hydrodynamics, and Ecosystem Profiles on the Mexican Caribbean Coast

Juan Carlos Alcérreca-Huerta ¹, Cesia J. Cruz-Ramírez ², Laura R. de Almeida ², Valeria Chávez ^{2,*}
and Rodolfo Silva ²

¹ Departamento de Observación y Estudio de la Tierra, la Atmósfera y el Océano, Consejo Nacional de Ciencia y Tecnología (CONACYT-ECOSUR), Chetumal 77014, Mexico; jcalcerreca@conacyt.mx

² Instituto de Ingeniería, Universidad Nacional Autónoma de México, Mexico City 04510, Mexico; ccruzr3@gmail.com (C.J.C.-R.); lauraribas.a@gmail.com (L.R.d.A.); rsilvac@iingen.unam.mx (R.S.)

* Correspondence: vchavez@iingen.unam.mx

Abstract: The interconnections between hydrodynamics, coastal sediments, and ecosystem distribution were analysed for a ~250 km strip on the northern Mexican Caribbean coast. Ecosystems were related to the prevailing and extreme hydrodynamic conditions of two contrasting coastal environments in the study area: Cancun and Puerto Morelos. The results show that the northern Mexican Caribbean coast has fine and medium sands, with grain sizes decreasing generally, from north of Cancun towards the south of the region. Artificial beach nourishments in Cancun have affected the grain size distribution there. On beaches with no reef protection, larger grain sizes ($D_{50} > 0.46$ mm) are noted. These beaches are subject to a wide range of wave-induced currents (0.01–0.20 m/s) and have steeper coastal profiles, where sediments, macroalgae and dune-mangrove systems predominate. The coastline with the greatest amount of built infrastructure coincides with beaches unprotected by seagrass beds and coral reefs. Where islands or coral reefs offer protection through less intense hydrodynamic conditions, the beaches have flatter profiles, the dry beach is narrow, current velocities are low (~0.01–0.05 m/s) and sediments are finer ($D_{50} < 0.36$ mm). The results offer a science-based description of the interactions between physical processes and the role played by land uses for other tropical coastal ecosystems.

Keywords: sediment transport; sedimentary environments; ecosystem distribution; coastal dynamics; coastal profiling; physical processes; anthropogenic pressure



Citation: Alcérreca-Huerta, J.C.; Cruz-Ramírez, C.J.; de Almeida, L.R.; Chávez, V.; Silva, R. Interconnections between Coastal Sediments, Hydrodynamics, and Ecosystem Profiles on the Mexican Caribbean Coast. *Land* **2022**, *11*, 524. <https://doi.org/10.3390/land11040524>

Academic Editor: Richard C. Smardon

Received: 9 March 2022

Accepted: 2 April 2022

Published: 4 April 2022

Publisher's Note: MDPI stays neutral with regard to jurisdictional claims in published maps and institutional affiliations.



Copyright: © 2022 by the authors. Licensee MDPI, Basel, Switzerland. This article is an open access article distributed under the terms and conditions of the Creative Commons Attribution (CC BY) license (<https://creativecommons.org/licenses/by/4.0/>).

1. Introduction

The enormous biodiversity of coastal ecosystems in the tropics has long been appreciated and is now recognised scientifically. However, mangroves, foredunes, beaches, seagrass meadows and coral reefs are all currently subject to environmental degradation aggravated by anthropogenic drivers, extreme hydrometeorological events, and climate warming [1–3]. Coastal dynamics are influenced by the ecosystems that exist in any locality. They affect the morphology, sediment transport, and sediment features of the environment where they are found.

Coral reefs enhance wave dissipation [4], as do seagrass meadows. This, in turn, contributes to sedimentation and the entrapment of sediment particles [5,6]. Dunes and beaches are interconnected by the wave energy that reaches the coastline [7,8] and the sediment budget along the beach profile [9]. Both beaches and dunes are also dependent on the characteristics of adjacent ecosystems [10–12].

The spatial arrangement of coastal ecosystems is associated with topo-bathymetric profile changes, waves, and currents, that are also linked with sediment transport patterns and sediment distribution [13]. Low hydrodynamic energy conditions promote the accumulation of fine sediments, whereas higher energy levels lead to coarse sediments [14]. Grain

size and sediment type contribute to shaping the coverage of submerged aquatic vegetation and its distribution. This contributes to reducing sediment transport capacity [15] and alters the flow dynamics [16,17] and the coastal morphology [18]. Thus, the complex interaction of hydrodynamics and sedimentary processes in coastal dynamics, under different sets of forcing conditions (waves, winds, tide, storm, etc.), affects the evolution of the environment [19].

In this regard, Gillies et al. [20] state that factors such as hydrodynamic energy and sedimentation, together with light availability, nutrient loads, and herbivore numbers are critical for the growth and establishment of tropical ecosystems (e.g., mangrove forests, seagrass beds and coral reefs).

Natural and anthropogenic changes impact directly on the two-way ecological–geomorphological linkages [21], and the stability of any ecosystem depends on the combination of the threats they face [22]. The resilience of coastal ecosystems is also dependent on physical maritime processes, geomorphology, and environmental characteristics, with coral reef-seagrass-mangrove systems being more resilient than open beaches with dune-mangrove systems [23]. For example, a study in Belize [12] showed that the presence of coral reefs, seagrass meadows and mangroves together, substantially moderates incoming wave energy, inundation levels and loss of mud sediment. They also found that, although mangroves alone can offer the coastal protection services mentioned, corals and seagrasses also influence the nearshore wave climate.

In the Caribbean, the coastal biodiversity is modulated by calm wave and wind conditions for most of the year, with extreme events of short duration from time to time (i.e., hurricanes and tropical storms) [23,24]. During these storms, currents can cause significant sediment transport, resulting in coastal erosion and accumulation [25]. Temporal and spatial distribution patterns of sediment, textural variations and biophysical characteristics of ecosystems, alongshore and cross-shore, provide information on coastal hydrodynamics [26].

On the northern Mexican Caribbean coast, tourist destinations, such as Cancun and the Riviera Maya, have been built along the coastal strip of sandy beaches, interspersed with a few low-lying rocky coastal terraces. However, the attractiveness of the area has been negatively affected by the impacts of increasing anthropisation, including both tourism and urban infrastructure. This has caused fragmentation and degradation of ecosystems, as well as disassociation from traditional and sustainable practices [27]. A range of studies on the distribution of marine ecosystems and sediment analysis (e.g., [28,29]), or hydrodynamics and sediment transport features in this area, are available. Tools such as numerical modelling [18] and statistical trend analysis [30] have also been used to improve the understanding of the hydro-sedimentary processes, including temporal and seasonal variations. More recent work in the northern Mexican Caribbean by [23,31,32] has related hydrodynamics to ecosystems, describing their fragmentation, distribution, systemic interactions, connectivity and resilience. However, analyses using detailed data are still required to improve the understanding of coastal behaviour.

This paper aims to analyse the connection between hydrodynamics (average and extreme conditions), sediments and ecosystems along the northern Mexican Caribbean coast. Wave climate, sediments and the distribution of coastal ecosystems were examined with a focus on two morphodynamically different beaches, one with, and the other without, coral reefs and seagrass meadows. The physical properties of 228 coastal sediment samples from the area, collected between 2005 and 2018, and kept at the Institute of Engineering, UNAM, were analysed. In addition, two contrasting coastal environments in the area, Cancun and Puerto Morelos, were analysed for a more comprehensive description of their sediment distribution and ecosystem profiles in relation to coastal hydrodynamic behaviour, for which numerical modelling was performed.

2. Materials and Methods

2.1. Study Area

The study area is in the Mexican state of Quintana Roo, along ~250 km of the northern Mexican Caribbean coast, between Cabo Catoche in the north (21.60583° N, 87.10334° W) and Punta Allen in the south (19.7976° N, 87.47430° W) (Figure 1). Mangroves, foredunes, beaches, seagrass meadows and coral reefs interact along the coast, forming a complex ecological system that influences the flow of matter and marine energy on the very narrow continental shelf [33,34]. Between Cancun and Tulum, the main touristic corridor in Mexico covers ~220 km² of the coastal zone. Most of the population and infrastructure in Quintana Roo are concentrated here [31]. It has 913,179 inhabitants and had an annual population growth rate of ~2.54% by 2015 [35]. In this area, scores of tourist developments of varying size alternate with urbanised areas such as Cancun, Puerto Morelos, Playa del Carmen, Akumal and Tulum (Figure 1a).

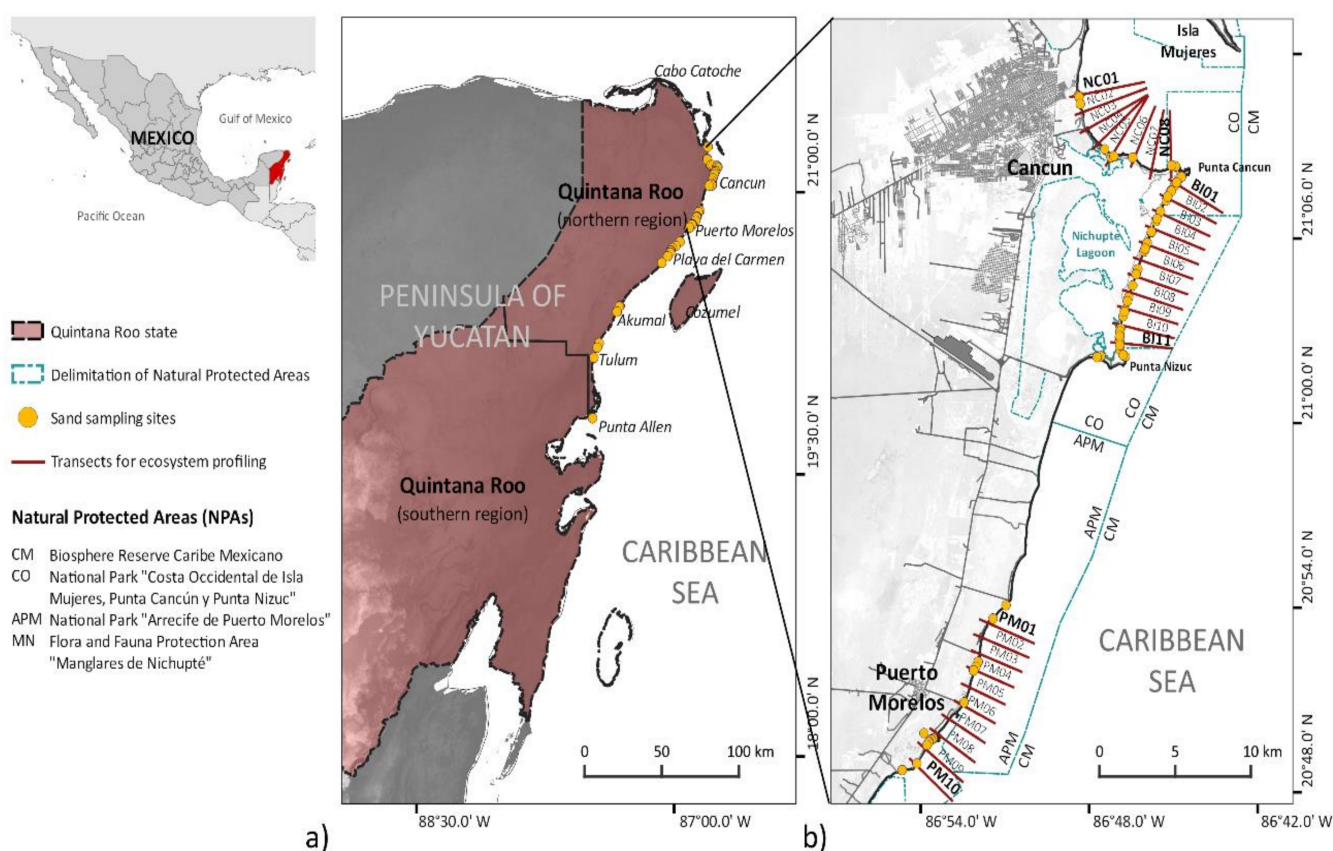


Figure 1. (a) Study area in the state of Quintana Roo, Mexico, and location of sand sampling sites. **(b)** Transects for coastal ecosystem profiling, sand sampling sites and surrounding Natural Protected Areas at the case study locations of Cancun and Puerto Morelos.

The area is affected by hurricanes and tropical storms that induce strong waves, winds, and coastal flooding in the summer months [36,37]. Trade winds also affect the area, as well as intense winds from the north. The microtidal conditions have a tidal range of 0.16–0.25 m [38]. Parallel to the coast, ocean currents flow with a southwest-northeast direction parallel to the deviation of the Yucatan landmass [39], but the nearshore currents, generated by the trade winds, produce southerly, littoral currents with a longshore sediment drift to the south [40].

In front of the Quintana Roo shore, a series of discontinuous coral reefs run parallel to the coast, particularly between Tulum and Puerto Morelos. These are part of the Mesoamerican Reef System, and form shallow coastal lagoons separating the reef from the

shoreline [41]. The reef lagoons have sandy bottoms usually covered by seagrass meadows. The dominant foundation species is *Thalassia testudinum*, along with *Syringodium filiforme* or *Halodule wrightii* and algae [42]. The combination of coral reefs, shallow reef lagoons and seagrass meadows provides most of the coast with natural protection by dissipating wave energy, producing a less hydrodynamic, sheltered, stable shoreline [11,12,43]. However, the international tourist resort of Cancun differs from other areas as there are no coral reefs and reef lagoons offshore, so the beach receives the direct impact of waves, making it more dynamic and variable than other beach areas [34,44].

Many protected areas and natural parks have been established along the Mexican Caribbean but, again, the beach front at Cancun is the exception (Figure 1b). The barrier island, between Punta Cancun and Punta Nizuc, separates the sea from the Bojorquez-Nichupte lagoon system, an important leftover section of wetland (Figure 1b). Over the last 50 years there has been massive tourism development over the former dunes, and canalisation of the lagoon inlets.

2.2. Sampling Techniques, Numerical Modelling and Data Analysis

2.2.1. Regional Analysis

Sand samples were collected in the study area from 2005 to 2018. The sampling sites were ~1 km apart, with special focus on beaches that have different types of coastal ecosystems and degrees of anthropisation, such as Cancun, Puerto Morelos, Playa del Carmen, Akumal and Tulum (Figure 1a). At each site, three sand samples were taken; at the backshore, foreshore and at a water depth of 0.5 m. A total of 228 sand samples were collected, of which 54.3%, 20.2%, and 13.6% were from Cancun, Puerto Morelos and Playa del Carmen, respectively. Most of the sand samples were from 2006–2007 (56.6%), with 15.8% taken in 2010, following the beach nourishment projects in Cancun subsequent to the impacts of Hurricane Wilma in 2005 [34].

Grain size distribution, sphericity (SPHT) and shape factor (SF) were measured with a CAMSIZER P4 particle analyser based on a dynamic image analysis method for particle size identification and the Krumbein–Sloss chart for particle shape parameters [45]. A pycnometer method was used to determine the specific gravity and density of sand samples. A descriptive statistical analysis of grain size (D_{10} , D_{50} and D_{90}), SPHT, SF and density is presented for all the sand samples in the study area.

The variation in the grain size, D_{50} , as a function of the longshore distance (D_{LS}) was analysed, taking the most northerly location in the study area, Costa Mujeres (21.24112° N, 86.80213° W), as a reference point, to Punta Allen in the south (19.79760° N, 87.47430° W). This information allows changes in the mechanical properties of sediments to be identified and the determination of any possible directions of sediment transport along the coastline [46,47].

Wave climate conditions were examined using the output dataset from hourly estimates of wave parameters from ERA5 reanalysis at the location 21.0° N, 86.5° W from 1979 to 2021 [48]. The ERA5 dataset provides wave climate conditions over a regular latitude-longitude global grid, with spatial spacing of 0.5°, and with the selected location being the most suitable for the analysis of wave climate conditions in the northern region. Wave rose diagrams and density histograms of wave height and wave period were produced to define the wave height (H_S), wave period (T) and wave direction (θ) under prevailing and extreme wave conditions for further numerical modelling. Extreme wave-conditions were defined considering an h_{crit} threshold, exceeded for a minimum period of 12 h, with h_{crit} being 1.5 times the annual average significant wave height based on the existing hourly records of wave climate conditions ($h_{crit} = 1.5 H_{S, annual}$) [49].

The spatial distribution of coastal environments in northern Quintana Roo was assessed for a coastal strip, 5 km from the shoreline, using an existing ecosystem classification (i.e., mangrove, coastal dunes, coral reefs, seagrass and macroalgae) obtained from [31,50,51]. The areas covered by human settlements, including their number of inhabitants, were also included, based on [52,53]. Considering the length of each beach, the

ecosystem and human settlement densities were calculated for Cancun, Puerto Morelos, Playa del Carmen, Akumal and Tulum.

2.2.2. Local-Scale Analysis

Cancun and Puerto Morelos were taken as specific case studies due to their contrasting coastal morphology, hydrodynamics and coastal ecosystem types (Figure 1b). The spatial grain size distribution for 150 m wide strips on the shore for both cases was assessed through the interpolation of D_{50} -values, to obtain the cross-shore distributions of grain sizes. The raster of interpolated D_{50} -values for each location was overlaid with the numerically modelled wave-induced currents, for prevailing and extreme wave events.

The WAPO model [54] was used to obtain the surface wave propagation and the wave-induced currents in the two areas. This model couples the REF/DIF model [55] to resolve the parabolic form of the mild slope equation including wave refraction-diffraction effects in intermediate waters [55,56]. Using the REF/DIF results, the WAPO model calculates the wave-induced currents by resolving the long wave equations. The numerical domains were defined as 20.79–20.91° N and 86.94–86.82° W (14.5 km × 18.4 km) for Cancun, and 21.01–21.27° N, 86.84–86.70° W (12.6 km × 13.0 km) for Puerto Morelos. The bathymetric information for the numerical domains was based on data from nautical charts of the Mexican Navy (SM 900; SM922; SM 922.1; SM 922.3) [57], bathymetric data from WorldView-2 satellite images [50], and local bathymetries obtained in 2008 and 2010. Both numerical domains were discretised in regular grids of 20-m spatial resolution.

Using the available topo-bathymetry data and including information on their coastal ecosystems, 19 beach profiles were assessed for Cancun, perpendicular to the coastline, and 10 for Puerto Morelos, each with a spacing of 1 km. For Cancun there were two areas of profiles: those north of Cancun and those on the barrier island. The classification detailed anthropised areas (urbanisation, hotel development, population, and roads), natural areas (subaerial vegetation other than mangroves), bodies of water (coastal lagoons), mangroves, coastal dunes, type of coast (beach, cliffs or rocky shoreline and artificial protection structures), seagrass and macroalgae, sediment accumulation and coral reefs. The profiles extend 500 m landward from the shore. On the seaside, the profiles extend up to a water depth of 20 m, depending on the information available on the coastal ecosystems. The length of each ecosystem in each profile was obtained through the intersection between the geographical position of the ecosystems, mangrove, reef, seagrass/macroalgae [50,51] and dunes [31], as well as the location of urban infrastructure, the type of coastline and water bodies [52,53]. The identification of the ecosystems in each section was also corroborated with Google Earth satellite images. Subsequently, the extension of each ecosystem in the profile was obtained and its sedimentary and hydrodynamic characteristics were associated with it.

Characteristic profiles were developed to provide a summary of the distinctive features that are shared between all profiles within a specific area of the case studies and to visualise the typical extent and distribution of coastal environments easily. Each profile was normalised by dividing the cross-shore distances (D_{CS}) by the total length of each profile (L) to obtain unit length profiles with the normalised cross-shore distance (D_{CS}^*) given by Equation (1).

$$D_{CS}^* = \frac{D_{CS}}{L} \quad (1)$$

In this way, the topo-bathymetric information could be averaged to produce two characteristic unit profiles for Cancun and one for Puerto Morelos. The ecosystem type within the characteristic unit profile was found from the statistical mode of the ecosystems at each corresponding location (D_{CS}^*) in the unit profiles. The normalised length of the characteristic profile was then scaled, using the average length of the n -profiles considered (i.e., $L_{AV} = \Sigma L_i / n$, with L_{AV} as the scale factor), to give the three characteristic profiles for the ecosystems in each case study.

3. Results

3.1. Sediments, Wave Climate, and Coastal Environment

3.1.1. Sediment Characterisation

Table 1 shows the sediment features from all the sand samples examined and individually for the case studies. The coefficients of variation (CoV) based on the standard deviation and the mean describe low regional variation (CoV < 13.3%) for the density, SF, and SPHT, but not for the grain size distribution for which variation is higher (CoV > 48.4%).

Table 1. Grain size (D_{10} , D_{50} and D_{90}), density, shape factor and sphericity for the sand samples from the study area.

Variable	Regional Results				^a Case Studies	
	Min.	Max.	Mean	Std. Dev.	Cancun	Pto. Morelos
Grain size, D_{10} [mm]	0.050	0.727	0.219	0.106	0.254	0.214
Grain size, D_{50} [mm]	0.093	1.433	0.391	0.200	0.451	0.368
Grain size, D_{90} [mm]	0.196	4.754	0.875	0.702	0.992	0.754
Density [kg/m^3]	1632	3232	2443	324	2565	2393
Shape factor, SF = b/L [-]	0.653	0.744	0.692	0.018	0.693	0.693
Sphericity, SPHT [-]	0.679	0.897	0.831	0.029	0.836	0.832

^a The values provided correspond to the mean values of each variable in the case study areas.

Most of the samples were calcareous deposits of biogenic origin. However, higher density values ($3232 \text{ kg}/\text{m}^3$) were found at backshore sites close to the rocky points of Punta Cancun and Punta Nizuc. In contrast, lower density sediment samples were found at Tulum, $1632 \text{ kg}/\text{m}^3$, possibly related to the porous calcite content in the samples. The SF and SPHT show values associated with fine and medium beach sands. The highest SPHT-values were for the northern beaches of Cancun, with SPHT > 0.87.

The grain size distribution in the study area was 0.219–0.875 mm for the mean values of D_{10} and D_{90} . However, less than 25% of the sand samples had a D_{50} < 0.219 mm or a D_{50} > 0.875 mm. Sampling sites in the northern part of Cancun and at Punta Brava had a wide sediment distribution, with D_{90} -values of 4.562 and 4.754 mm, respectively, which correspond to granular sediment and pebbles. On the other hand, sediment with >10% silt was found in Punta Allen, where D_{10} < 0.0627 mm. Less than 5% of the sand samples had such extreme values of grain size distribution.

Table 1 shows the differences between the case studies of Cancun and Puerto Morelos. The grain size distribution (D_{50} and D_{90}), density and SPHT in Puerto Morelos were lower than that of the region, the opposite of Cancun, where the sediment features were higher than in the region as a whole.

Findings worth noting are two sand samples from Cancun (Figure 2): a 2005 sample from Cancun, before the beach nourishment, and a sand sample from the same location, but after the beach nourishment. The first sample showed a remarkable degree of well-sorted sediment, as seen in Figure 2a, and a D_{90} = 0.436 mm and a D_{10} = 0.252 mm, both close to the D_{50} = 0.317 mm, giving one of the most homogeneous grain size distributions of all the sand samples collected. In contrast, the second samples showed similar sand parameters but a significantly higher grain size distribution and a low degree of sorting (Figure 2b). With this great difference in the grain size distributions, it is to be expected that the morphodynamic behaviour of the beach under present conditions is different than before the beach nourishment.

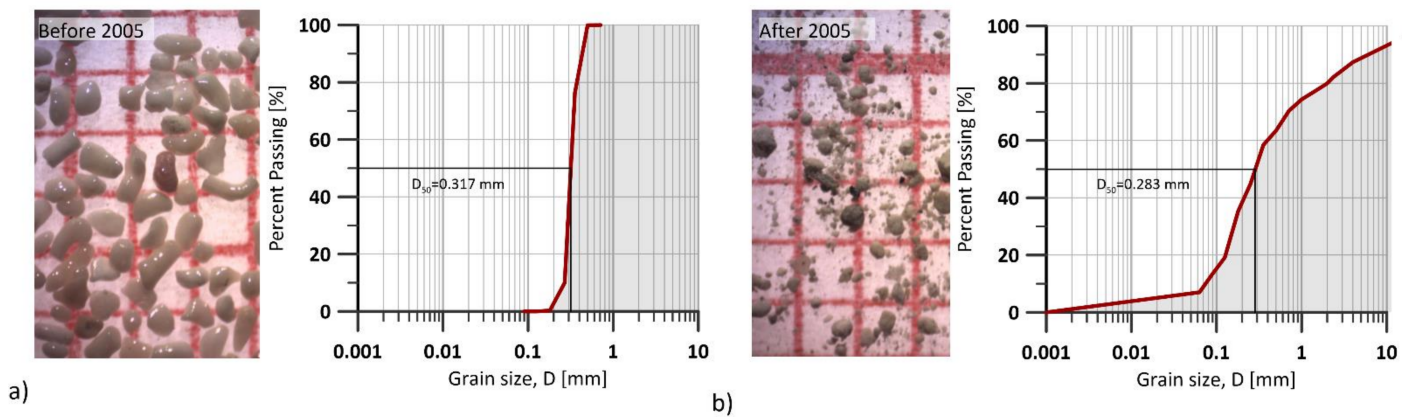


Figure 2. Cumulative grain size distribution and microscope images (1 mm grid) of sand samples at Cancun (21.172913° N, 86.805336° W) (a) before and (b) after the 2005 beach nourishments in that area following hurricane Wilma.

Changes in sediment grain size for each of the three parts on the beach profiles are given in Figure 3. The coarsest backshore sands were from the southern half of the Cancun barrier island, with a grain size $0.430 < D_{50} < 0.747$ mm for ~69.0% of the sand samples. In contrast, 26.6% of the sand samples in the north of Cancun had a grain size of over 0.430 mm. Although some peaks in the grain size were seen at specific sites, such as Punta Brava ($D_{50} = 0.616$ at $D_{LS} = 61.3$ km), north of Playa del Carmen ($D_{50} = 0.483$ at $D_{LS} = 79.1$ km), and at Akumal ($D_{50} = 0.631$ at $D_{LS} = 139.2$ km), there was generally a decrease in grain size towards the south, for nearshore, foreshore and backshore samples (Figure 3a–c). The finest sands were from the backshore at Tulum ($D_{LS} = 169.4$ km) and Punta Allen ($D_{LS} = 221.1$ km) with $D_{50} < 0.101$ mm.

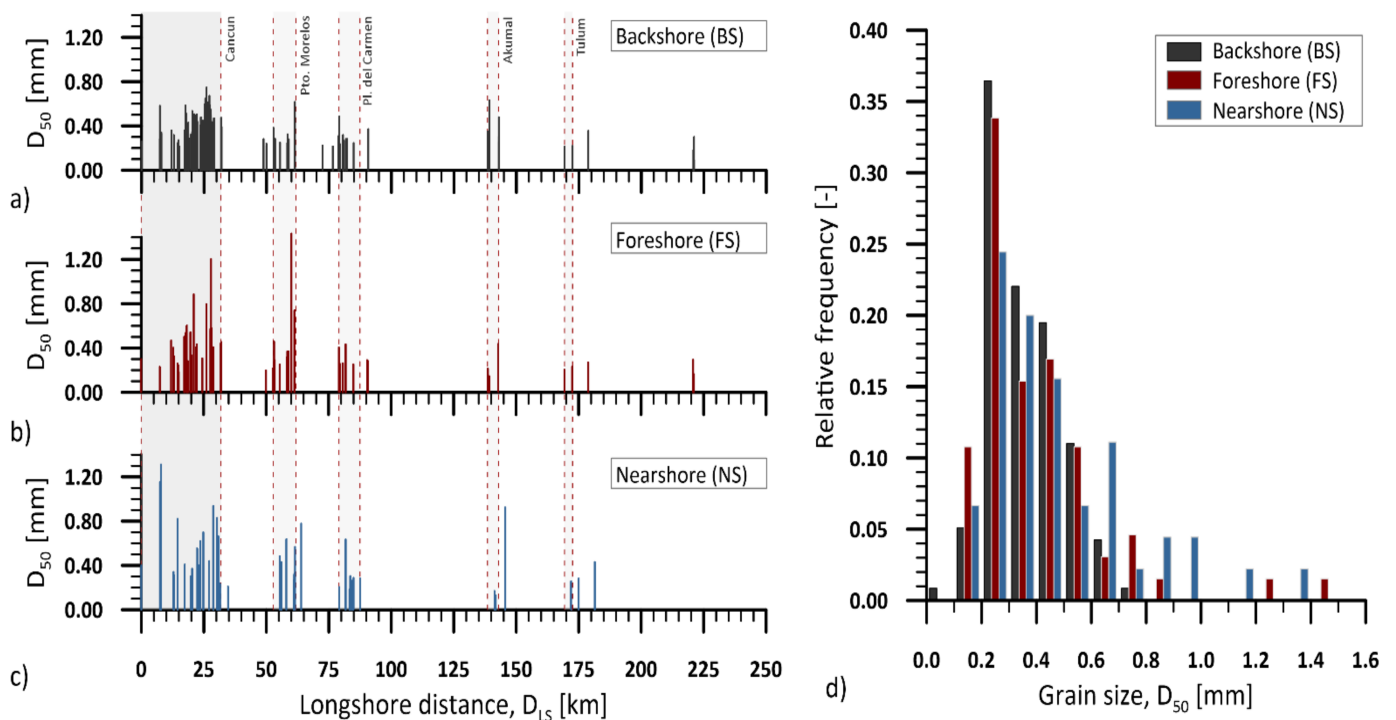


Figure 3. Grain size variations for the different beach profile sections: (a) BS, (b) FS and (c) NS. The zero-reference point D_{LS} is at 21.24112° N, 86.80213° W, with DLS values increasing parallel to the coast and in a southerly direction. (d) Histogram for the grain size distribution for the different parts of the profiles for all the sample sites.

The grain size distribution in the foreshore and nearshore samples showed medium to fine sands, with a grain size that had higher D_{50} -values than those of the backshore (Figure 3d). The nearshore had the largest grain size ($D_{50,mean} = 0.464 \pm 0.26$ mm) with a wider variation along the coast. This was followed by the foreshore ($D_{50,mean} = 0.401 \pm 0.23$ mm) and backshore ($D_{50,mean} = 0.358 \pm 0.13$ mm). About 13.45% of the nearshore sand samples exceeded $D_{50} = 0.800$ mm; however, this percentage decreased to 4.6% for the foreshore and to zero for the backshore.

The coarsest sands on the northern Mexican Caribbean were from specific sites in Cancun and Punta Brava ($D_{LS} = 7.89$ km and $D_{LS} = 61.3$ km), regardless of which part of the beach profile they were taken from. In summary, fine to very coarse sands were found on the northern Mexican Caribbean coast, according to the Udden–Wenworth grain size scale, with a predominance of fine and medium sand, with 75% of sands having $D_{50} < 0.479$ mm.

3.1.2. Wave Climate Conditions

The most frequent wave climate in the area between 1979 and 2020 had waves with a predominant ESE–WNW direction ($\theta = 112.5^\circ$) (Figure 4a). Nearly 95.5% of the waves had heights of $H_S < 2.0$ m, of which 41.7% were of $H_S < 1.0$ m, with peak wave periods of $TP = 4.0$ – 8.0 s. The period of prevailing wave $TP = 6.0$ s had an individual probability of occurrence $> 10\%$. About 4.5% of the waves were over $H_S = 2$ m and only 0.3% of the wave height exceeded $H_S = 3$ m in the prevailing wave conditions.

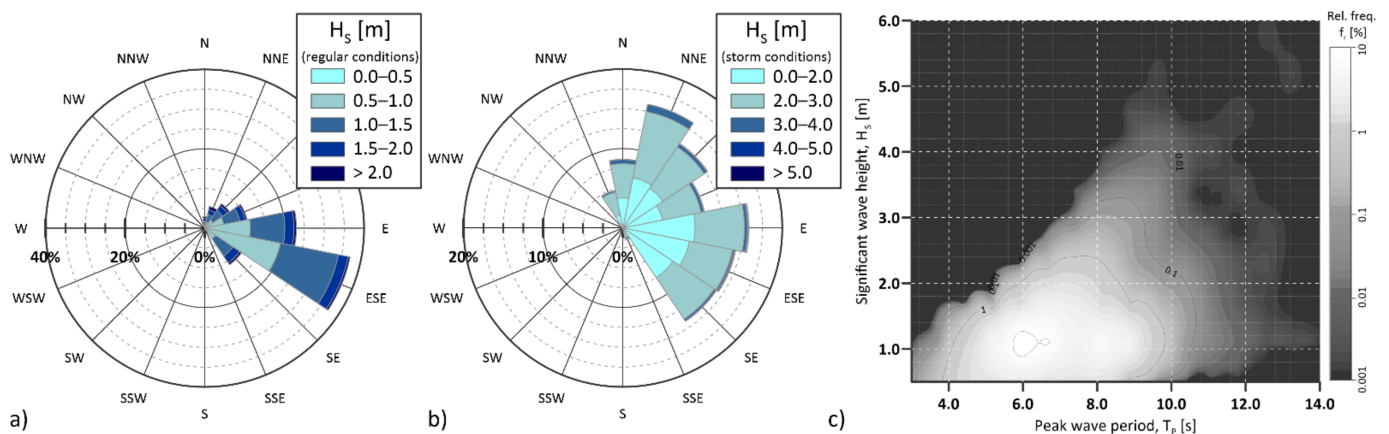


Figure 4. Wave rose diagrams for incident waves in (a) prevailing and (b) extreme conditions. (c) Bivariate histogram of H_S and T_P for wave climate conditions from ERA5 at 21.0° N, 86.5° W.

For extreme wave conditions, the critical wave height threshold was $h_{crit} = 1.71$ m. Wave heights were above this threshold, but below 2.0 m for 48.8% of the storm conditions, whereas 46.5% were $2.0 < H_S < 3.0$ m (Figure 4b). Severe conditions, with $H_S > 3.0$ m, occurred 4.7% of the time, with waves coming mainly from a NNE direction ($\theta = 22.5^\circ$) and up to $H_S = 11.28$ m, associated with wave periods of $TP = 7$ – 8 s. Therefore, extreme wave conditions for the numerical modelling of wave propagation in the case studies were defined for a critical condition of $H_S = 3.0$ m, $\theta = 22.5^\circ$ (Figure 4b) and a $TP = 8.0$ s (Figure 4c).

The average storm data for every five-year period is shown in Table 2, including the mean storm duration, total number of storms, and the yearly averaged minima and maxima within the period. The maximum significant wave height reached within the quinquennial period is also provided.

The average wave height was $H_{S-AV} = 2.04 \pm 0.02$ m with wave periods of $TP = 7$ – 8 s. Maximum wave heights of $H_{S-Max} = 10.67$ m and $H_{S-Max} = 11.28$ m were recorded with Hurricane Gilbert (1988, H5) and Hurricane Wilma (2005, H4), respectively, which made landfall in the north of the peninsula. Other very energetic waves were associated with hurricanes that approached without making landfall on the peninsula (e.g., hurricanes

Allen 1980, H5; Ivan 2004, H5; and Michael, H1). In addition, the maximum wave heights in 1991 and 1995 occurred in stormy, not hurricane conditions.

Table 2. Mean and maximum wave height during extreme wave conditions, storm duration and number of storms for every five-year period.

Period	Wave Height		Storm Duration [h]			Number of Storms		
	H _{S-AV} [m]	^a H _{S-Max} [m]	Mean	^a Min	^a Max	Mean	^a Min	^a Max
1980–1985	2.03	7.43 (1980)	35.2	31.4 (1984)	39.3 (1981)	19.8	14 (1982)	25 (1980)
1985–1990	2.04	11.28 (1988)	35.5	29.0 (1985)	41.3 (1989)	19.8	14 (1986)	26 (1988)
1990–1995	2.04	4.02 (1991)	39.0	31.4 (1992)	44.0 (1990)	17.0	14 (1992)	22 (1990)
1995–2000	2.06	5.69 (1995)	46.3	31.3 (1995)	55.2 (1999)	22.0	14 (1997)	28 (1996/1998)
2000–2005	2.03	7.13 (2004)	36.6	30.5 (2001)	45.5 (2004)	21.6	19 (2000)	28 (2001)
2005–2010	2.08	10.67 (2005)	38.7	31.9 (2007)	44.1 (2008)	23.6	21 (2006)	27 (2007)
2010–2015	2.02	4.28 (2014)	34.2	31.9 (2013)	37.4 (2012)	22.2	17 (2011/2012)	33 (2010)
2015–2020	2.03	3.71 (2018)	37.7	26.7 (2016)	53.4 (2015)	21.8	17 (2019)	29 (2016)
	Average		37.9	30.5	45.0	21.0	16.3	27.3

^a The year of occurrence is given in parentheses.

The duration of storms was variable, with no clear pattern, being generally of between 30.5 and 45.0 h, with maximums in 1999 and 2015. For 1995–2000 the duration of storms was longer than for other periods, up to 46.3 h. The historical minimum for the number of storms per year was reached in 1982, 1986, 1992, and 1997 (14), with a variable average storm duration, while in 2010 and 2016, there were more storms than in other years, but with low persistence.

In general, there has been a trend to more storminess, with the maximum number of storms, 22–26 in 1980–1995, increasing to 27–28 for 1995–2010 and up to 33 after 2010. There has also been a rise in the minimum number of storms in a year, from 14 before 2000 to more than 17 after 2010.

3.1.3. Land Use

The main characteristics of land use in the ~250 km coastal trip from Cabo Catoche to Punta Allen are shown in Table 3. Of these, about 31.8, 9.0, 8.4, 4.4 and 3.1 km of the anthropised waterfront of Cancun, Puerto Morelos, Playa del Carmen, Akumal and Tulum, respectively, were examined in more detail (see Figure 1a). The coastal tourist corridor, from Cancun to Tulum, has 79.4% of the total population living in the coastal area of the Mexican Caribbean, of which 96.4% live in Cancun and Playa del Carmen (i.e., 780,882 inhabitants).

An area of 22,544 ha of the study area is covered by mangroves, with the most extensive being between Cabo Catoche and northern Cancun (in the north), and between Tulum and Punta Allen (in the south). Cancun has a large area of mangrove, with a density similar to that of Puerto Morelos, but 4–10 times higher than that of Playa del Carmen, Tulum or Akumal. Coastal dunes are virtually absent in the anthropised areas analysed. Seagrass and macroalgae are also present in the northern region, with a similar density to that found off Cancun and Puerto Morelos, but far lower than off Playa del Carmen, Akumal and Tulum. The coral reefs are a discontinuous ecosystem, most dense between the south of Punta Nizuc (Cancun) and Puerto Morelos, and with some sections, such as the urban/tourist zone of Cancun, where there are no reef remnants.

Table 3. Characteristics of land use in the northern Mexican Caribbean.

^a Variable		Northern Region	Anthropized Areas in the Northern Region				
			Cancun	Pto. Morelos	Pl. del Carmen	Akumal	Tulum
Inhabitants	total per km	818,876 (3276)	630,959 (19,842)	9188 (1021)	149,923 (17,848)	1310 (293)	18,233 (5881)
Human settlements	ha	17,313	11,803	186	3543	36	386
	ha/km	(69)	(371)	(21)	(422)	(8)	(125)
Mangrove	ha	22,544	3153	1055	212	41	29
	ha/km	(90)	(99)	(117)	(25)	(9)	(9)
Coastal dune	ha	1719	27	15	8	—	0.1
	ha/km	(7)	(1)	(2)	(1)	—	(0.0)
Seagrass and macroalgae	ha	33,327	4381	1222	642	203	254
	ha/km	(133)	(138)	(136)	(76)	(46)	(82)
Coral reefs	ha	4589	123	237	47	51	50
	ha/km	(18)	(4)	(26)	(6)	(12)	(16)

^a Hectares (1 ha = 10,000 m²) and the density in hectares per kilometre of coastline (ha/km).

3.2. Case Studies

The detailed results for Cancun and Puerto Morelos are used to show the links between beach sediments features, wave climate and land use, in a local-scale analysis. The chosen locations mainly differ in the presence, and lack of, a fringing reef, as well as the extent of urban infrastructure nearby.

The wave-induced currents and grain size variation in the sediments are described, along with the land use spatial distribution and their associated beach profiles. For each location, two scenarios were modelled using the wave climate results for the northern Mexican Caribbean for: a) prevailing wave conditions with $H = 1.0$ m, $T = 6.0$ s and ESE direction ($\theta = 112.5^\circ$), and b) extreme conditions with $H = 3.0$ m, $T = 8.0$ s and NNE direction ($\theta = 22.5^\circ$).

3.2.1. Case Study 1: Cancun

For Cancun, the land use, distribution of sediment grain size and wave induced currents, with their velocity, magnitude and direction, are shown in Figure 5. In Figure 5a land use and bands showing grain size variations are shown, while Figure 5b shows currents induced by prevailing waves, and Figure 5c shows these currents in extreme waves.

The southern section of the beach in Cancun ($\sim 21.04\text{--}21.06^\circ$ N) has the coarsest sediment found in the case study (Figure 5a). Another area with coarse sediment is the central part of the barrier island ($\sim 21.10^\circ$ N). A proxy of sediment transport paths can be inferred, as they normally run from areas of coarse material towards zones with finer sediments, resulting in a south-north direction in the north of the beach ($\sim 21.10^\circ$ N to $\sim 21.13^\circ$ N) and a north-south direction in the south of the beach ($\sim 21.04^\circ$ N to $\sim 21.06^\circ$ N). This observed sediment transport path is closely related to the wave-induced currents under prevailing conditions (Figure 5b), where the magnitude along the barrier island (~ 0.05 m/s) increases close to the shoreline and at the nearshore, allowing the settlement of coarse particles (>0.600 mm), according to the Hjulström curve. Under extreme conditions, there is a dominant north-south direction along the barrier island with velocities >0.20 m/s (Figure 5c) that, based on the Hjulström curve, might lead to erosional processes which might modify the prevailing sediment distribution in the area. It is worth noting that, although the wave-induced currents are small, even under extreme conditions (<0.3 m/s), they can still induce transport and erosional processes for the grain sizes found in the study area.

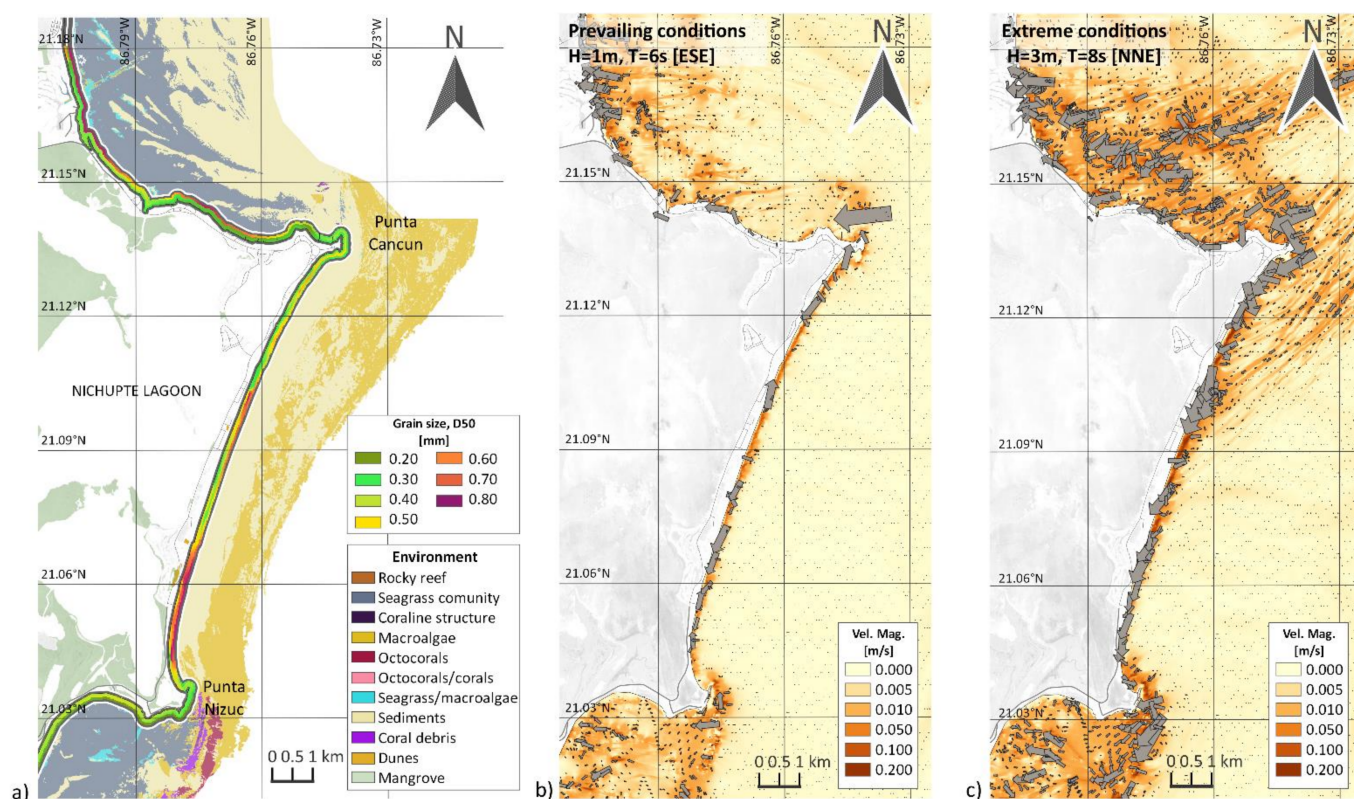


Figure 5. Results for Cancun showing (a) land use and variation of the sediment grain size (D_{50}). Sediment grain size variation is shown for a 150 m width strip along the shoreline, with sand samples from the backshore, nearshore and foreshore zones. Speed and direction of wave-induced currents are also shown for (b) prevailing [$HS = 1$ m, $TP = 6$ s, $\theta = 112.5^\circ$ (ESE)] and (c) extreme conditions [$HS = 3$ m, $TP = 8$ s, $\theta = 22.5^\circ$ (NNE)].

The medium and coarse sands observed in the south of the barrier island ($D_{50} > 0.40$ mm) are among the coarsest sand samples in the northern Mexican Caribbean. This could be linked to the wave-induced currents, but also to the possible degradation of a lithified Pleistocene dune located at $\sim 21.06^\circ$ N, that extends over the Nichupte Lagoon, and that could be submerged seaward (Figure 5a). Between the two areas of coarse sediment on the barrier island, there is an area of finer material near to a coastal dune (Playa Delfines). This material is of the finest grain size found in the study area with $D_{50} = 0.154$ mm and $D_{50} = 0.169$ mm at the dune crest and the berm, respectively. This sediment is possibly becoming a reservoir that can be transported to other beach segments under extreme wave conditions.

Sediment and macroalgae are the main bottom cover on the submerged beach of the barrier island of Cancun. The coarse sands found here are linked to intense currents very close to the shoreline, where most of the wave-energy dissipation and continuous high turbulent velocities due to wave breaking are expected to occur. At ~ 21.11 – 21.13° N, under extreme conditions, the velocity magnitude increases close to the shore, with velocity magnitudes of >0.05 m/s spreading seaward, over patches of sediment interspersed with areas of macroalgae. There are low velocity magnitudes (<0.010 m/s) over the sediment and macroalgae in front of the barrier island (Figure 5) where the greater water depth lessens the impact of the waves.

The wave-induced currents around Punta Nizuc flow southwards due to the diffraction of the waves by the rocky point. The higher velocities develop close to the corals, possibly related to turbulence and wave breaking. In the reef lagoon south of Punta Nizuc, velocity magnitudes of ~ 0.010 m/s develop over a wide area of backreef, induced by the shallower water in the reef lagoon. Finer sediments in the shoreline were found as the

velocity magnitudes decrease over the shoreline. Mangroves coincide where there is finer sediment and where seagrass communities are also found.

In the northern part of the beach of Cancun, the dominant bottom covers are seagrass and sedimentary deposits, which give rise to submarine dunes. Over these, in prevailing conditions, velocity magnitudes (<0.05 m/s) increase, especially at 21.15 – 21.18° N, induced by the shallower waters. Sediment size is greater at the nearshore ($D_{50} > 0.800$ mm), and finer sediment is found in the backshore. This area coincides with the development of seagrass meadows and macroalgae patches. The wave-induced currents from Punta Cancun, with a W-E direction, follow the longitudinal direction of the submarine dunes over the seagrass areas. This effect is also seen in extreme conditions, with the wave-induced currents being more intense at the transition between areas of seagrass and sediments. This is because the sedimentary deposits lie at depths about 1 m less than where seagrass meadows are found. It is important to mention that the wave propagation model does not consider wave energy attenuation from seagrass meadows, nor from coral reefs, so that the currents reaching the coast could be less strong than those indicated by the model.

Isla Mujeres is located near the northern beaches of Cancun (Figure 1). This island provides shelter from wave effects, thereby decreasing the intensity with which sediment is transported. In the long term, this protection may have created the conditions that explain why the northern part of Cancun has shallower waters, as it produces a less dynamic area, where sediment can be deposited. Nowadays, wave diffraction-refraction processes could lead to the wave-induced currents observed in Cancun's northern beaches. Similarly, the island could induce the conditions needed for the establishment of seagrass meadows—waters with low turbidity, sheltered from waves. Once they have become established, seagrasses decrease wave power and current energy, increase sedimentation and fix bottom sediments, due to the structure of their leaves, roots and rhizomes [6,58,59]. The protected conditions of the northern beaches could also explain the reduction in grain size compared to that of the barrier island.

The beach profiles are shown in Figures 6 and 7, where the distribution of coastal ecosystems, their segmentation, and land use in the north of Cancun (NC), and on the barrier island (BI), are detailed.

The anthropised areas in the subaerial profiles are about 210–235 m in width. The maximum anthropised width is ~ 424 m, at NC02, limited by terrestrial or marine water bodies and occupying the entire subaerial portion of the profile. On the barrier island, the maximum extent of anthropised areas is ~ 344 m, also limited by water bodies.

The profiles for northern Cancun (NC01 to NC08) show mangroves and seagrass communities. The latter are present in all the submarine profiles, covering 8.4–52.1% of the profile length. There are no coral structures in the northern part of Cancun, nor in front of the barrier island, although south of Punta Nizuc, there is a coral reef community (Figure 5a). Off the barrier island, macroalgae covers 10.7–38.3% of the profile length, in combination with marine sediments (6.1–54.3%), and there are no seagrass meadows. Here, an average 35% of the profile length is marine sediments, but these could cover up to 2064 m of the sea bottom, as at BI03. It is worth noting that the presence of macroalgae on the seabed in front of the barrier island occurs at depths of over 10 m, except at profile BI11 (Punta Nizuc). Therefore, the drag and roughness effects of macroalgae on wave propagation are limited.

The data show that the subaerial landscape of Cancun barrier island is dominated by anthropised areas, mangrove ecosystems and water bodies. However, this barrier island was entirely composed of dunes prior to the large-scale tourist development of the 1970s, which practically eliminated dunes [34], leaving traces of the dune field [10]. Prior to the urbanisation, eroded beach sediment used to be recovered from dunes following extreme meteo-oceanographic conditions, a natural process that cannot occur nowadays [34].

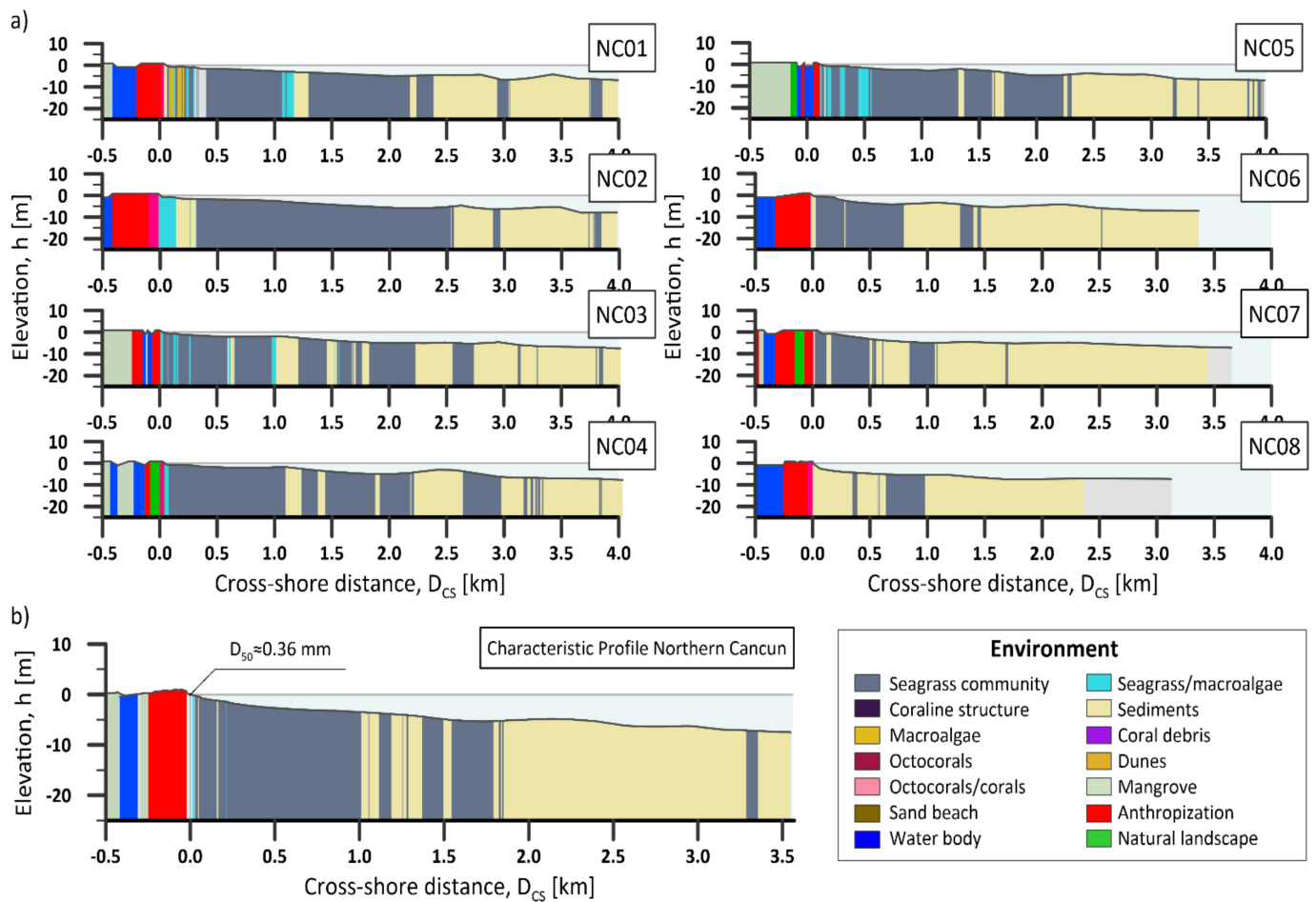


Figure 6. Beach profiles in northern Cancun, extending from 500 m inland, and up to 4 km seaward. The shoreline is located at a cross-shore distance $D_{CS} = 0$ m. The profiles (a) are numbered as in Figure 1. The land use for northern Cancun (b) corresponds to profiles NC01-NC08.

Almost all the coastal profiles at Cancun show sandy beaches, except NC03 and NC05. The beaches are 17.4 m wide, on average, in the north, and 45 m wide on the barrier island, with a maximum, BI09, of 65.9 m, where the only existing coastal dune is found and the greatest grain sizes (Playa Delfines). South of BI09, towards Punta Nizuc, the profiles also show mangrove areas, similar to the north of Cancun, with an average extent landward of ~170.5 m (i.e., ~34.1% of the subaerial landscape analysed). These mangrove areas are part of the Bojorquez–Nichupte lagoon system (Figure 1b). The connection between the lagoon and the sea is now limited to two rigidised inlets, meaning that the connectivity between the mangrove and the coastal zone, as well as the sediment balance once offered by intermittent inlets, has been drastically modified [34].

The characteristic beach profiles obtained for northern Cancun (Figures 6b and 8a) and the barrier island (Figures 7b and 8b) differ in their morphology and the ecosystems found. For the north of Cancun, the profile is mainly wide areas of shallow waters ($h < 10$ m at $0 < D_{CS} < 4$ km) where seagrass meadows predominate at cross-shore distances of 0–2 km, with marine sediments beyond. The effect of the shallow water contributes to the slight increase in wave-induced velocities here (~0.05 m/s). On the other hand, the subaerial profile for the barrier island is anthropised, and limited by the Nichupte Lagoon. The submarine part of the profile shows rapid deepening, with water depths of >10 m at a cross-shore distance of 500 m from the beach. Sandy beaches are found close to the shore, then marine sediments up to a cross-shore distance of ~950 m, beyond which there are macroalgae ecosystems.

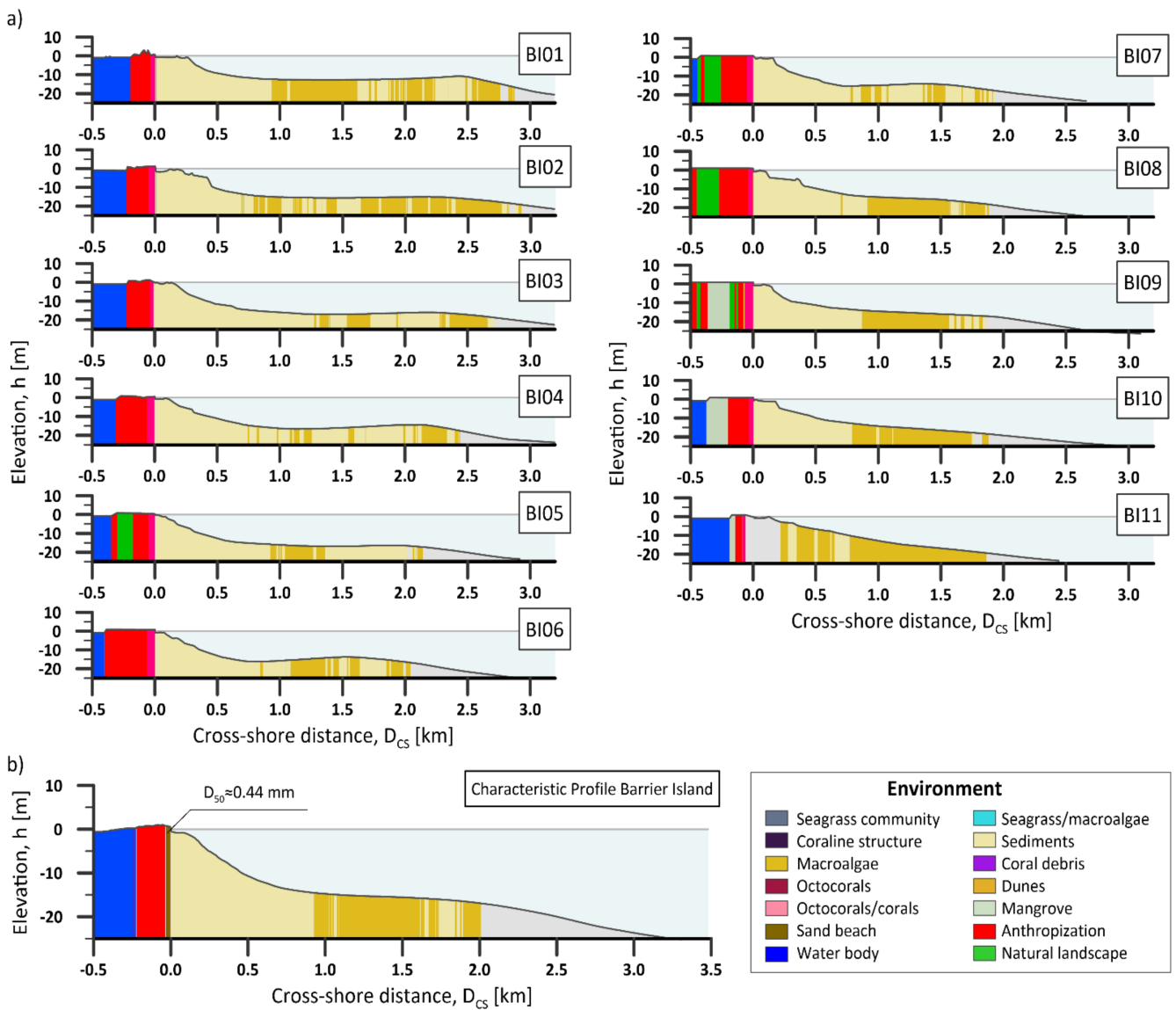


Figure 7. Beach profiles at the Cancun barrier island, extending from 500 m inland, towards a water depth of 20 m. The shoreline is located at a cross-shore distance $D_{CS} = 0$ m. The profiles (a) are numbered from north to south as in Figure 1. The land use on the Cancun barrier island (b) corresponds to profiles BI01-BI11.

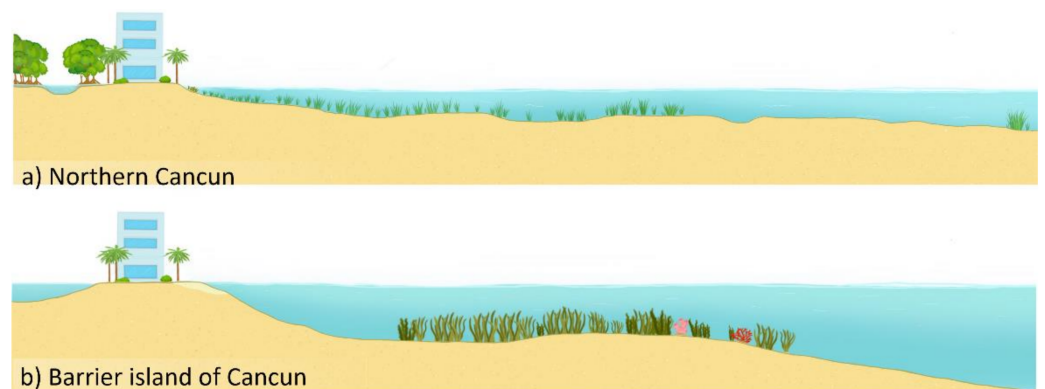


Figure 8. Schematisation of the distribution of coastal environments and characteristic coastal infrastructure at (a) northern Cancun and (b) the barrier island of Cancun.

3.2.2. Case Study 2: Puerto Morelos

Figure 9 shows the sediment grain sizes, land use and wave-induced currents for prevailing and extreme wave conditions along the Puerto Morelos coast. The effects of the nearby fringing reef are clear, with substantial changes in grain size, wave-induced currents and ecosystem distribution.

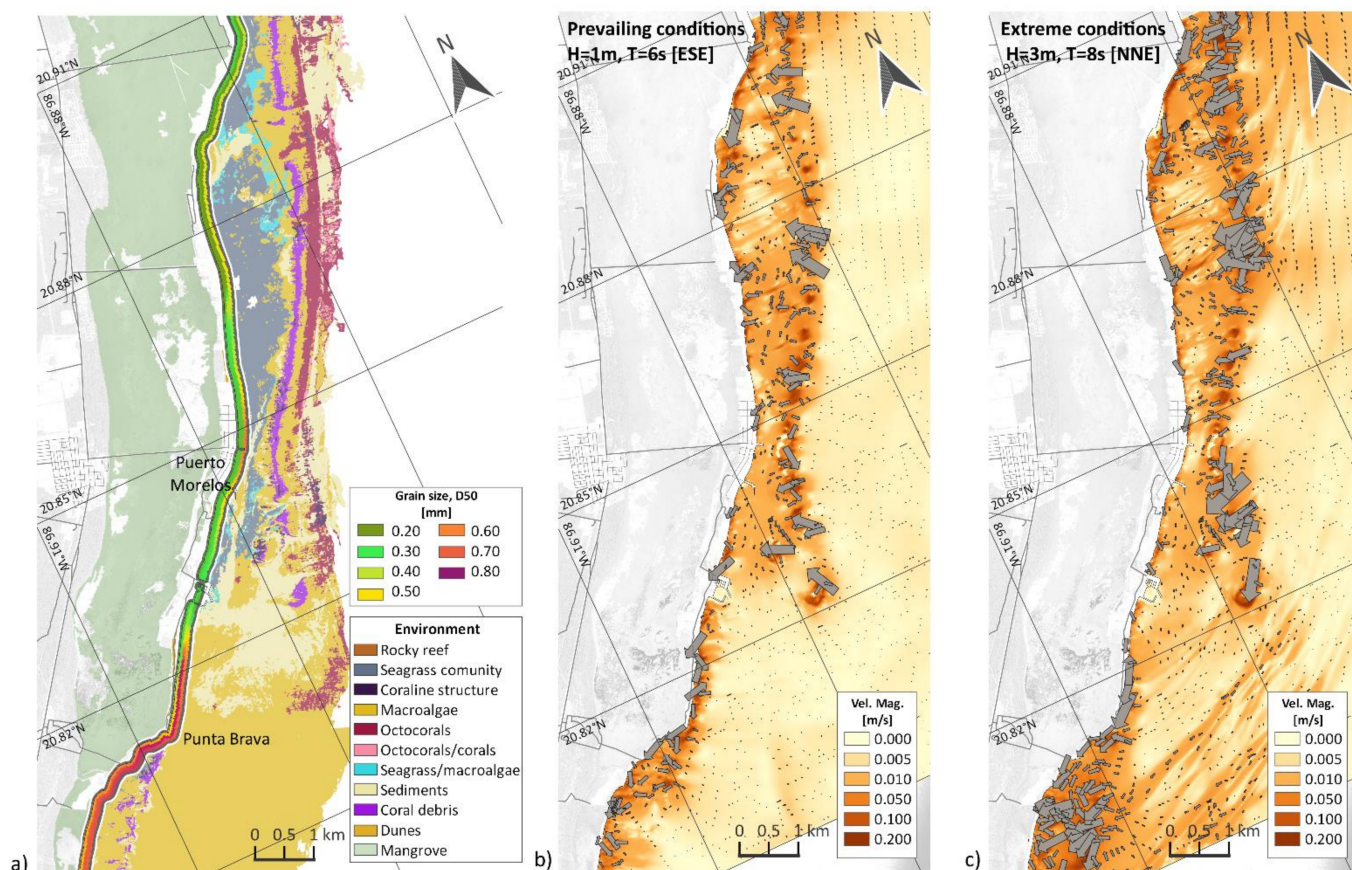


Figure 9. Results for Puerto Morelos showing (a) land use and variation of the sediment grain size (D_{50}). Sediment grain size variation is depicted over a strip of 150 m width along the shoreline considering sand samples at the backshore, nearshore and foreshore zones. The speed and direction of wave-induced currents is also shown for (b) prevailing [$HS = 1$ m, $TP = 6$ s, $\theta = 112.5^\circ$ (ESE)] and (c) extreme conditions [$HS = 3$ m, $TP = 8$ s, $\theta = 22.5^\circ$ (NNE)].

The highest velocities, >0.200 m/s, are where coral reef formations and coral debris are found, independent of wave conditions. Other areas with high velocities are seen where there is no reef, such as Punta Brava, where there is also an increase in the sediment grain size, $D_{50} > 0.750$ mm. Near to the town of Puerto Morelos, the backreef lagoon is narrower and the sediment grain size is greater at the nearshore. In the lee of the reef, seagrass communities and macroalgae are found, along with unvegetated areas of finer sediments, $D_{50} < 0.400$ mm. To the south, there are areas of submerged sediment where the velocity magnitude is low, less than ~ 0.005 m/s. In general, the unvegetated areas are not sheltered by reefs, but velocity magnitudes are low, which favours sediment deposition.

North of the town there is a wider area between the reef and the shore, where the velocity magnitudes are > 0.010 m/s. The sea bottom is mainly covered by seagrass and sediments (Figure 9a). Like northern Cancun, and in the reef lagoon south of Punta Nizuc, these velocities are lower than those impacting the shoreline where there is no wave protection from coral reefs (Figure 9b,c).

At open beaches, without reef protection (Figure 9a), there are large areas covered by macroalgae, similar to the beaches along the Cancun barrier island (Figure 5a). Macroalgae

settle in areas of low velocity magnitudes, <0.005 m/s in prevailing conditions (Figure 9b) and <0.050 m/s in extreme conditions.

In prevailing conditions, the wave-induced currents are perpendicular to the coral reef barrier. However, a longshore current is seen, close to the shoreline, with a north-south direction. The longshore current continues south to Punta Brava in both prevailing and extreme wave conditions. South of Punta Brava, in extreme wave conditions, a small area covered by coral debris and octocorals induces a very complex pattern of wave-induced currents, although the direction is predominantly southward.

In Puerto Morelos the extensive mangrove forests have no direct connection with the sea [60], which means that they do not directly influence the size of the sediment found on the beach. In the reef lagoon the small sediment grain size ($D_{50} < 0.300$ mm) is probably due to the seabed being covered by seagrass communities that are protected by the reefs (Figure 9).

The coastal profiling results for Puerto Morelos are given in Figure 10. In every profile all the ecosystems are represented, except for P10 in the southernmost part of Puerto Morelos, close to Punta Brava, where macroalgae is predominant. Mangrove forests cover ~ 5 – 12% of the length of each profile, about 275 m of the subaerial landscape. Inland, the mangrove area is almost continuous in all the profiles, only disrupted by anthropised areas, in general, with a cross-shore distance $0 < D_{CS} < 300$ m. In profiles P01–P08, the anthropisation lies next to the beach, with no buffer area (Figure 9a). Profiles P03 and P05–P07 have most anthropisation, ~ 200 – 310 m of the profile length, representing ~ 40 – 60% of the subaerial profile.

The dune ecosystem is minimal, 9.8 m on average, mainly in the south (P09 and P10), where it extends for up to 50 m. The foredunes at Puerto Morelos are ~ 4 m high and degraded in many areas due to the construction of infrastructure [33]. In contrast, all the profiles have sandy beaches, with an average width of ~ 17 m, increasing to 30–50 m northward, except for P08, where there are structures protecting the port infrastructure.

In the marine section of the profiles, macroalgae bottom cover predominates, with an average coverage of ~ 930 m, although in the south, macroalgae covers up to ~ 3050 m (P10). Marine sediments are common in the south, as shown in P07 to P09, providing an average coverage of ~ 465 m and reaching cross-shore distances of up to ~ 1110 m.

The seagrass communities are mostly between P02 and P07, with ~ 420 m on average, reaching a maximum in P02 and P03 of ~ 1 km. In contrast to the macroalgae ecosystems, seagrass communities are almost continuous, as can be observed in most of the profiles (e.g., P02 and P03). Coral reef structures, coral debris and octocorals cover distances of ~ 390.4 m on average, with octocorals being the most common, especially in P01 and P03, where they cover a cross-shore distance of up to 540 m. The fragmentation of the ecosystems is more pronounced in profiles P01, and P07 to P09 (close to the port), being usually interspersed with seagrass, corals and marine sediments. These profiles have the greatest land use segmentation with ~ 71 – 75 interwoven patches of different ecosystems, marine sediments and macroalgae being the most common.

The characteristic profile for Puerto Morelos is shown in Figures 10b and 11. The sub-aerial landscape is mainly composed of mangroves. Anthropised areas limited by the beach are the second most common land use (Figure 11). There is a narrow band of sediments, ~ 30 m, seaward from the shoreline, with a grain size of $D_{50} \approx 0.30$ mm, interspersed with areas of macroalgae and occasional seagrass patches. Seaward of $D_{CS} = 175$ m, a continuous area of seagrass communities predominates, but with segments of marine sediments and macroalgae intercepted. Beyond $D_{CS} = 880$ m, the predominant environment is macroalgae, interrupted by octocoral segments at $1650 < D_{CS} < 1850$ m, over the forereef, at water depths of 10 m. It is worth noting that coral debris and coralline structures form a mound in almost all profiles landward of the forereef (Figure 10a).

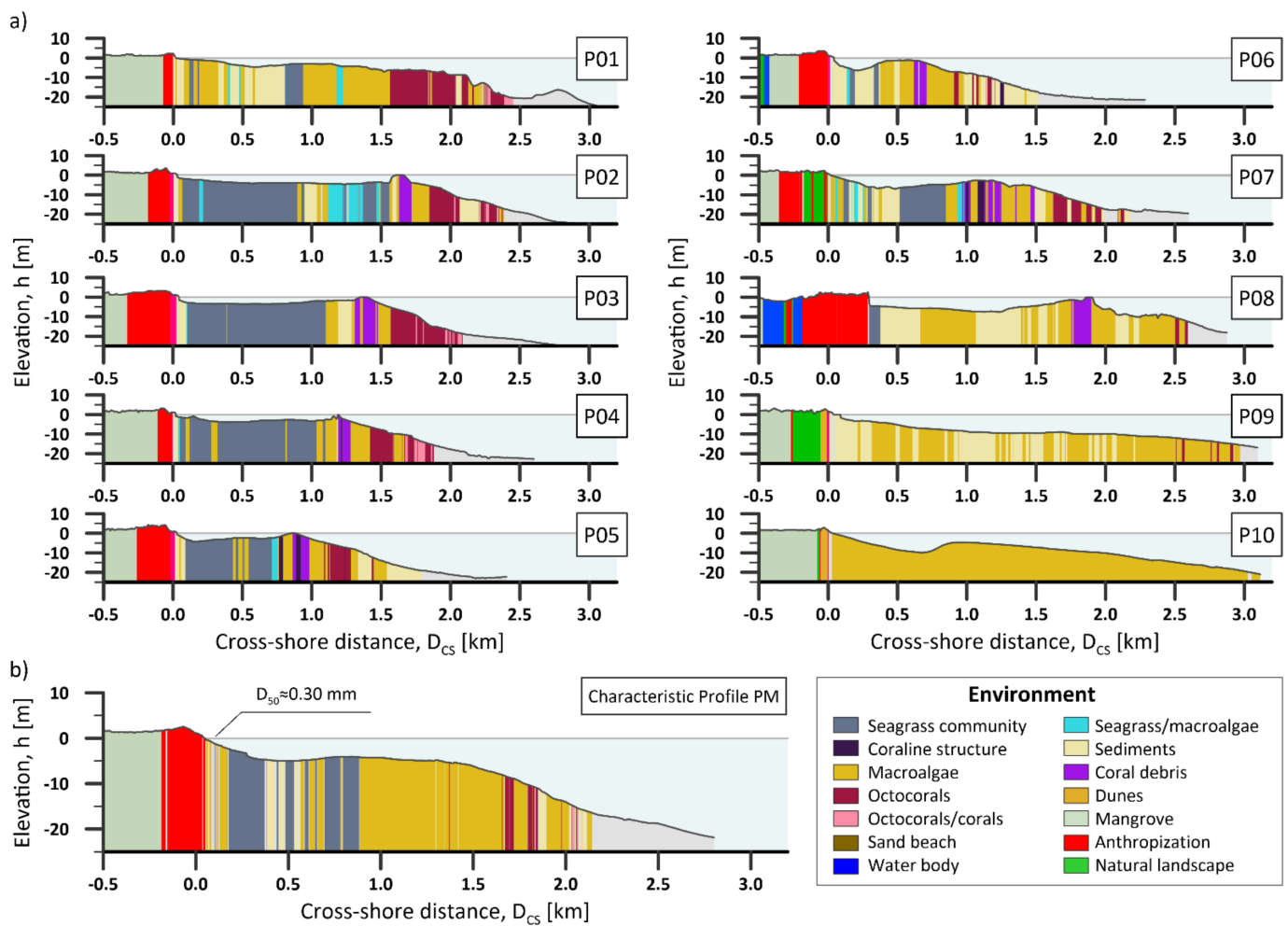


Figure 10. Beach profiles at Puerto Morelos (PM), extending from 500 m inland, towards a water depth of 25 m. The shoreline is located at a cross-shore distance $D_{CS} = 0$ m. The profiles (a) are numbered from north to south as in Figure 1. The land use at Puerto Morelos (b) corresponds to profiles P01–P10.



Figure 11. Schematisation of the distribution of coastal environments and characteristic coastal infrastructure at Puerto Morelos.

4. Discussion and Concluding Remarks

The dynamics of any coast involve a complex exchange of matter and energy that comes from continually changing ecological-geomorphological linkages. When evaluating the sedimentary characteristics of the northern Mexican Caribbean coast, it has been possible to verify that, on a large spatial scale, the sedimentary flow is from north to south. However, at local scale, the evaluation of detailed coastal dynamics, characteristics of coastal ecosystems (types and extent) and land uses is essential to understand the complex and interconnected relationships between these factors and local geomorphology.

The evaluation of case studies at a local level has shown that coastlines that are hydrodynamically protected by islands or coral reefs have shallow, flatter profiles created

by sedimentation. This protection also contributes to the development of seagrass meadows. The interconnectivity between coral reefs and seagrasses is recognised: coral reefs dissipate the force of currents and wave energy through breaking and bottom friction [61], creating a suitable environment for seagrass. In turn, the seagrasses control turbidity and nutrients, providing water conditions that encourage the growth of coral reefs [62]. Since seagrasses also attenuate currents and waves, sediment particles are deposited in the reef lagoon, so that, over time, a shallow area develops that further contributes to wave attenuation [63]. This condition has been verified in Puerto Morelos. As a consequence, backshore/foreshore sediments are finer (~0.2–0.3 mm), dry beaches are narrower (~17 m) and more stable [44], with smaller foredunes [10] than nearby areas without this protection. In the study area north of Cancun, despite not presenting a barrier reef but with the protection of Isla Mujeres, similar geomorphological characteristics have been found, mainly due to shallow and flat nearshore, dominated by seagrasses. In these study cases, the characteristics of the profile are related to coastal ecosystem development. However, despite the extensive mangrove areas in Puerto Morelos, they seem not to be linked to hydro-sedimentary dynamics. This is because they are basin forest mangroves, a very specific type of mangrove that are not directly connected to the coastal zone [23,60]. For a better understanding of these relationships and their influence on the morphodynamics of the beaches affected by the ecosystems, the different values of bottom friction should be included in hydrodynamic models, depending on the various bottom covers (reef, sediment, seagrass, algae), so advanced models capable of making this type of evaluation are recommended.

On the other hand, beaches unprotected by seagrass and coral reefs, as found on the barrier island of Cancun, have large grain sizes (D_{50} ~0.4 mm), wider beaches (~45 m) and have high dunes. These conditions are associated with steep, deep coastal profiles dominated by interspersed segments of sediment and macroalgae. Since macroalgae induce little wave friction and turbulence, their effect on reducing sediment transport is limited, as well as their capacity for sediment retention [43]. In these cases, the characteristics of the beach profile basically depend on the characteristics of the available sediment and the energy of the waves [64]. Foredunes are important ecosystems, especially on the exposed beaches, as they act as a buffer to flooding and coastal erosion, as well as serving as a sediment reservoir. However, the degradation of these ecosystems, seen most clearly on the barrier island of Cancun, means that this environmental service has been lost. Building on the dune area of exposed beaches interrupts the dynamic interaction between the dunes, beach and foreshore. As a result, the coastal profile steepens, the sediment coarsens, the habitat for seabed vegetation deteriorates, the wave attenuating effect of the vegetation vanishes, the coast becomes more exposed, and vulnerability to extreme wave climate events increases, developing into a vicious cycle of environmental deterioration that directly impacts human activities and livelihoods.

The northern Mexican Caribbean coast is exposed to both natural and human disturbances that affect the spatial distribution of sediments, hydrodynamics and ecosystem health, which shape the coastal landscape. This area is predominantly urban, with anthropogenic pressures on the environment, often fractioning subaerial ecosystems (e.g., coastal dunes), submerged aquatic vegetation and coral reefs. Water pollution, infrastructure development or water-based tourism activities are among the pressure drivers in the region [10,41,65]. These cause the coastal ecosystems to be unable to perform their primary functions, reducing their resilience in episodic or chronic events, and thereby decreasing their capacity to protect the coast, and increasing their vulnerability to extreme events and climate change [66,67]. For example, the artificial beach nourishments in Cancun have affected grain size distribution there. According to the analysis of the large sediment samples collected, no changes to sedimentary or environmental features over time were seen. However, the information presented might serve as a baseline for future comparisons.

Global and local changes in frequency, persistence and intensity of atmospheric and marine conditions seem to be outpacing the adaptive capacity of ecosystems. A growing storm number was identified for the northern Mexican Caribbean; therefore, further study

is recommended to strengthen the analysis of wave conditions at locations near to the region and indices that reflect anomalies in climate patterns. In tropical coastal zones, long periods of calm allow ecosystems to establish, recover and mature, while extreme-event-induced pulses allow species turnover and simultaneous hydrodynamic interconnection of neighbouring ecosystem. Through the morphodynamic study of two beaches on the Mexican Caribbean that are close geographically, but have very different environments, it is possible to highlight the strong interrelationships between hydrodynamics, land use and sedimentation processes.

Through the use of information associated with sediment characteristics and land use (e.g., coastal ecosystems, human occupation data), spatial and cross-sectional representations of the study area of these three-dimensional connections and anthropogenic pressures have allowed us to identify trends in the coastal dynamics that may improve the coastal management of the beaches studied. Continuous monitoring might provide hard evidence of spatial and temporal changes in coastal dynamics, hydro-sedimentary processes, and the effects of natural and human disturbances [68]. Long-term monitoring of wave climate conditions, sediment and environmental changes is important, as seen in Cancun, where changes in the grain size distribution testify to the human intervention from beach nourishments following Hurricane Wilma in 2005.

Finally, tourism in the Caribbean is based on the sun, sea and sand concept. Its sustainability is dependent on the health of the ecological environment and the balance between anthropised areas and open beaches. Therefore, the use of green infrastructure for adaptive coastal management must be based on an understanding and diagnosis of the state of the interconnections of these ecosystems.

Author Contributions: Conceptualization, J.C.A.-H., C.J.C.-R., L.R.d.A., V.C. and R.S.; methodology, J.C.A.-H., C.J.C.-R., L.R.d.A. and V.C.; software, V.C. and R.S.; validation, J.C.A.-H., C.J.C.-R., L.R.d.A., V.C. and R.S.; formal analysis, J.C.A.-H., C.J.C.-R. and L.R.d.A.; investigation, J.C.A.-H., C.J.C.-R., L.R.d.A. and R.S.; resources, R.S.; data curation, J.C.A.-H. and C.J.C.-R.; writing—original draft preparation, J.C.A.-H., C.J.C.-R. and L.R.d.A.; writing—review and editing, V.C. and R.S.; visualisation, J.C.A.-H. and C.J.C.-R.; supervision, J.C.A.-H. and R.S.; project administration, R.S.; funding acquisition, R.S. All authors have read and agreed to the published version of the manuscript.

Funding: The APC was funded by CEMIE-Océano (CONACYT -SENER-Fondo de Sustentabilidad Energética project: FSE-2014-06-249795 “Centro Mexicano de Innovación en Energía del Océano CEMIE-Océano”).

Data Availability Statement: Restrictions apply to the availability of the sedimentological data. This data was obtained from Instituto de Ingeniería, UNAM and is available from the authors with the permission of Instituto de Ingeniería, UNAM. Further datasets are available at [50] and [53].

Acknowledgments: The authors would like to acknowledge the access to the sand sample collection and database of the Instituto de Ingeniería, UNAM. Acknowledgements are given to the CONACYT (Consejo Nacional de Ciencia y Tecnología) program ‘Investigadoras e Investigadores por México’ project 761. The program of postdoctoral grants from DGAPA-UNAM for the third author is also recognised.

Conflicts of Interest: The authors declare no conflict of interest. The funders had no role in the design of the study; in the collection, analyses, or interpretation of data; in the writing of the manuscript, or in the decision to publish the results.

References

1. Hughes, T.P.; Barnes, M.L.; Bellwood, D.R.; Cinner, J.E.; Cumming, G.S.; Jackson, J.B.C.; Kleypas, J.; van de Leemput, I.A.; Lough, J.M.; Morrison, T.H.; et al. Coral reefs in the Anthropocene. *Nature* **2017**, *546*, 82–90. [[CrossRef](#)] [[PubMed](#)]
2. Larcombe, P.; Costen, A.; Woolfe, K.J. The hydrodynamic and sedimentary setting of nearshore coral reefs, central Great Barrier Reef shelf, Australia: Paluma Shoals, a case study. *Sedimentology* **2001**, *48*, 811–835. [[CrossRef](#)]
3. van den Hoek, L.S.; Bayoumi, E.K. Importance, destruction and recovery of coral reefs. *IOSR J. Pharm. Biol. Sci.* **2017**, *12*, 59–63. [[CrossRef](#)]
4. Sheppard, C.; Dixon, D.J.; Gourlay, M.; Sheppard, A.; Payet, R. Coral mortality increases wave energy reaching shores protected by reef flats: Examples from the Seychelles. *Estuar. Coast. Shelf Sci.* **2005**, *64*, 223–234. [[CrossRef](#)]

5. Christianen, M.J.A.; van Belzen, J.; Herman, P.M.J.; van Katwijk, M.M.; Lamers, L.P.M.; van Leent, P.J.M.; Bouma, T.J. Low-canopy seagrass beds still provide important coastal protection services. *PLoS ONE* **2013**, *8*, e62413. [[CrossRef](#)]
6. Maxwell, P.S.; Eklöf, J.S.; van Katwijk, M.M.; O'Brien, K.R.; de la Torre-Castro, M.; Boström, C.; Bouma, T.J.; Krause-Jensen, D.; Unsworth, R.K.F.; van Tussenbroek, B.I.; et al. The fundamental role of ecological feedback mechanisms for the adaptive management of seagrass ecosystems—A review. *Biol. Rev.* **2017**, *92*, 1521–1538. [[CrossRef](#)]
7. Cohn, N.; Hoonhout, B.; Goldstein, E.; De Vries, S.; Moore, L.; Durán Vinent, O.; Ruggiero, P. Exploring marine and aeolian controls on coastal foredune growth using a coupled numerical model. *J. Mar. Sci. Eng.* **2019**, *7*, 13. [[CrossRef](#)]
8. Pellón, E.; de Almeida, L.R.; González, M.; Medina, R. Relationship between foredune profile morphology and aeolian and marine dynamics: A conceptual model. *Geomorphology* **2020**, *351*, 106984. [[CrossRef](#)]
9. Delgado-Fernandez, I. Meso-scale modelling of aeolian sediment input to coastal dunes. *Geomorphology* **2011**, *130*, 230–243. [[CrossRef](#)]
10. de Almeida, L.R.; Silva, R.; Martínez, M.L. The relationships between environmental conditions and parallel ecosystems on the coastal dunes of the Mexican Caribbean. *Geomorphology* **2022**, *397*, 108006. [[CrossRef](#)]
11. Franklin, G.; Mariño-Tapia, I.; Torres-Freyermuth, A. Effects of reef roughness on wave setup and surf zone currents. *J. Coast. Res.* **2013**, *165*, 2005–2010. [[CrossRef](#)]
12. Guannel, G.; Arkema, K.; Ruggiero, P.; Verutes, G. The power of three: Coral reefs, seagrasses and mangroves protect coastal regions and increase their resilience. *PLoS ONE* **2016**, *11*, e0158094. [[CrossRef](#)] [[PubMed](#)]
13. Golshani, A.; Baldock, T.E.; Mumby, P.J.; Callaghan, D.; Nielsen, P.; Phinn, S. Climate impacts on hydrodynamics and sediment dynamics at reef islands. In Proceedings of the 12th International Coral Reef Symposium, James Cook University, Townsville, Australia, 9–13 July 2012.
14. Elfrink, B.; Baldock, T. Hydrodynamics and sediment transport in the swash zone: A review and perspectives. *Coast. Eng.* **2002**, *45*, 149–167. [[CrossRef](#)]
15. Liu, C.; Shen, Y. Flow structure and sediment transport with impacts of aquatic vegetation. *J. Hydrodyn.* **2008**, *20*, 461–468. [[CrossRef](#)]
16. Moki, H.; Taguchi, K.; Nakagawa, Y.; Montani, S.; Kuwae, T. Spatial and seasonal impacts of submerged aquatic vegetation (SAV) drag force on hydrodynamics in shallow waters. *J. Mar. Syst.* **2020**, *209*, 103373. [[CrossRef](#)]
17. Nakayama, K.; Shintani, T.; Komai, K.; Nakagawa, Y.; Tsai, J.W.; Sasaki, D.; Tada, K.; Moki, H.; Kuwae, T.; Watanabe, K.; et al. Integration of submerged aquatic vegetation motion within hydrodynamic models. *Water Resour. Res.* **2020**, *56*, 8. [[CrossRef](#)]
18. Amoudry, L.O.; Souza, A.J. Deterministic coastal morphological and sediment transport modeling: A review and discussion. *Rev. Geophys.* **2011**, *49*, RG2002. [[CrossRef](#)]
19. Storlazzi, C.D.; Elias, E.; Field, M.E.; Presto, M.K. Numerical modeling of the impact of sea-level rise on fringing coral reef hydrodynamics and sediment transport. *Coral Reefs* **2011**, *30*, 83–96. [[CrossRef](#)]
20. Gillis, L.; Bouma, T.; Jones, C.; van Katwijk, M.; Nagelkerken, I.; Jeuken, C.; Herman, P.; Ziegler, A. Potential for landscape-scale positive interactions among tropical marine ecosystems. *Mar. Ecol. Prog. Ser.* **2014**, *503*, 289–303. [[CrossRef](#)]
21. Stallins, J.A. Geomorphology and ecology: Unifying themes for complex systems in biogeomorphology. *Geomorphology* **2006**, *77*, 207–216. [[CrossRef](#)]
22. Perry, C.T.; Kench, P.S.; Smithers, S.G.; Riegl, B.; Yamano, H.; O'Leary, M.J. Implications of reef ecosystem change for the stability and maintenance of coral reef islands. *Glob. Chang. Biol.* **2011**, *17*, 3679–3696. [[CrossRef](#)]
23. Odériz, I.; Gómez, I.; Ventura, Y.; Díaz, V.; Escalante, A.; Gómez, D.T.; Bouma, T.J.; Silva, R. Understanding drivers of connectivity and resilience under tropical cyclones in coastal ecosystems at Puerto Morelos, Mexico. *J. Coast. Res.* **2020**, *95*, 128–132. [[CrossRef](#)]
24. Salazar-Vallejo, S.I. Huracanes y biodiversidad costera tropical. *Rev. Biol. Trop.* **2002**, *50*, 2.
25. Vincent, C.E.; Young, R.A.; Swift, D.J. Bed-load transport under waves and currents. *Mar. Geol.* **1981**, *39*, M71–M80. [[CrossRef](#)]
26. Klein, A.H.d.F.; Miot da Silva, G.; Ferreira, O.; Alveirinho-Dias, J. Beach sediment distribution for a headland bay coast. *J. Coast. Res.* **2005**, *42*, 285–293.
27. Murray, G. Constructing paradise: The impacts of big tourism in the Mexican Coastal Zone. *Coast. Manag.* **2007**, *35*, 339–355. [[CrossRef](#)]
28. Calva-Benítez, L.G.; Torres-Alvarado, R. Organic carbon and textural characteristics of sediments in areas with turtlegrass *Thalassia testudinum* in coastal ecosystems of the southeastern gulf of Mexico. *Univ. Ciencia. Tróp. Húmed.* **2011**, *27*, 133–144.
29. Ouillon, S. Why and how do we study sediment transport? Focus on coastal zones and ongoing methods. *Water* **2018**, *10*, 390. [[CrossRef](#)]
30. Poizot, E.; Anfuso, G.; Méar, Y.; Bellido, C. Confirmation of beach accretion by grain-size trend analysis: Camposoto beach, Cádiz, SW Spain. *Geo-Mar. Lett.* **2013**, *33*, 263–272. [[CrossRef](#)]
31. Guimaraes, M.; Zúñiga-Ríos, A.; Cruz-Ramírez, C.J.; Chávez, V.; Odériz, I.; van Tussenbroek, B.I.; Silva, R. The conservational state of coastal ecosystems on the Mexican Caribbean coast: Environmental guidelines for their management. *Sustainability* **2021**, *13*, 2738. [[CrossRef](#)]
32. Silva, R.; Martínez, M.L.; van Tussenbroek, B.I.; Guzmán-Rodríguez, L.O.; Mendoza, E.; López-Portillo, J. A framework to manage coastal squeeze. *Sustainability* **2020**, *12*, 610. [[CrossRef](#)]
33. Franklin, G.L.; Torres-Freyermuth, A.; Medellín, G.; Allende-Arandia, M.E.; Appendini, C.M. The role of the reef–dune system in coastal protection in Puerto Morelos (Mexico). *Nat. Hazards Earth Syst. Sci.* **2018**, *18*, 1247–1260. [[CrossRef](#)]

34. Martell-Dubois, R.; Mendoza, E.; Mariño-Tapia, I.; Odériz, I.; Silva, R. How effective were the beach nourishments at Cancun? *J. Mar. Sci. Eng.* **2020**, *8*, 388. [CrossRef]
35. SEGOB-COESPO. *Atlas Sociodemográfico Quintana Roo*. Available online: <https://qroo.gob.mx/index2.php/segob/coespo/atlas-sociodemografico> (accessed on 1 December 2021).
36. Jáuregui, E. Climatology of landfalling hurricanes and tropical storms in Mexico. *Atmósfera* **2003**, *16*, 193–204.
37. Ojeda, E.; Appendini, C.M.; Mendoza, E.T. Storm-wave trends in Mexican waters of the Gulf of Mexico and Caribbean Sea. *Nat. Hazards Earth Syst. Sci.* **2017**, *17*, 1305–1317. [CrossRef]
38. Kjerfve, B. Tides of the Caribbean Sea. *J. Geophys. Res.* **1981**, *86*, 4243. [CrossRef]
39. Cetina, P.; Candela, J.; Sheinbaum, J.; Ochoa, J.; Badan, A. Circulation along the Mexican Caribbean coast. *J. Geophys. Res. C Ocean.* **2006**, *111*, C8. [CrossRef]
40. Kjerfve, B. *Coastal Oceanographic Characteristics: Cancun-Tulum Corridor, Quintana Roo*; ECOMAR-EPOMEX: Campeche, Mexico, 1994.
41. Rioja-Nieto, R.; Álvarez-Filip, L. Coral reef systems of the Mexican Caribbean: Status, recent trends and conservation. *Mar. Pollut. Bull.* **2019**, *140*, 616–625. [CrossRef]
42. Jordán-Dahlgren, E.; Rodríguez-Martínez, R.E. The Atlantic coral reefs of Mexico. In *Latin American Coral Reefs*; Cortés, J., Ed.; Elsevier: Amsterdam, The Netherlands, 2003; pp. 131–158, ISBN 9780444513885.
43. James, R.K.; Silva, R.; van Tussenbroek, B.I.; Escudero-Castillo, M.; Mariño-Tapia, I.; Dijkstra, H.A.; van Westen, R.M.; Pietrzak, J.D.; Candy, A.S.; Katsman, C.A.; et al. Maintaining tropical beaches with seagrass and algae: A promising alternative to engineering solutions. *Bioscience* **2019**, *69*, 136–142. [CrossRef]
44. Mariño-Tapia, I.; Enríquez-Ortiz, C.; Silva, R.; Mendoza, E.; Escalante-Mancera, E.; Ruiz-Rentería, F. Comparative morphodynamics between exposed and reef protected beaches under hurricane conditions. *Coast. Eng. Proc.* **2014**, *1*, 55. [CrossRef]
45. Retsch Technology. *Operating Instructions/Manual. Particle Size Analysis System CAMSIZER*; Doc.Nr. CA.; Jenoptik Germany: Haan, Germany, 2007.
46. Anfuso, G.; Pranzini, E.; Vitale, G. An integrated approach to coastal erosion problems in northern Tuscany (Italy): Littoral morphological evolution and cell distribution. *Geomorphology* **2011**, *129*, 204–214. [CrossRef]
47. Frihy, O.E.; Dewidar, K.M. Patterns of erosion/sedimentation, heavy mineral concentration and grain size to interpret boundaries of littoral sub-cells of the Nile Delta, Egypt. *Mar. Geol.* **2003**, *199*, 27–43. [CrossRef]
48. Hersbach, H.; Bell, B.; Berrisford, P.; Biavati, G.; Horányi, A.; Muñoz-Sabater, J.; Nicolas, J.; Peubey, C.; Radu, R.; Rozum, I.; et al. ERA5 Hourly Data on Single Levels from 1979 to Present. Available online: <https://cds.climate.copernicus.eu/cdsapp#!/dataset/10.24381/cds.bd0915c6?tab=overview> (accessed on 3 January 2022).
49. Boccotti, P. *Wave Mechanics for Ocean Engineering*; Elsevier Science: Amsterdam, The Netherlands, 2000; ISBN 9780080543727.
50. Cerdeira-Estrada, S.; Martell-Dubois, R.; Heege, T.; Rosique-De La Cruz, L.O.; Blanchon, P.; Ohlendorf, S.; Müller, A.; Silva, R.; Mariño-Tapia, I.J.; Martínez-Clorio, M.I.; et al. *Cobertura Bentónica de los Ecosistemas Marinos del Caribe Mexicano: Cabo Catoche—Xcalak 2018*; Scale 1:4; Comisi' on Nacional para el Conocimiento y Uso de la Biodiversidad (CONABIO): Mexico City, Mexico, 2018.
51. CONABIO. *Distribución de los Manglares en México en 2020*; 1:50000; Comisión Nacional para el Conocimiento y Uso de la Biodiversidad (CONABIO): Mexico City, Mexico, 2020.
52. Cruz, C.J.; Mendoza, E.; Silva, R.; Chávez, V. Assessing degrees of anthropization on the coast of Mexico from ecosystem conservation and population growth data. *J. Coast. Res.* **2019**, *92*, 136. [CrossRef]
53. INEGI. *Mapa de Uso de Suelo y Vegetación*; 1:50000; Instituto Nacional de Estadística y Geografía: Mexico City, Mexico, 2017.
54. Silva, R.; Baquerizo, A.; Losada, M.Á.; Mendoza, E. Hydrodynamics of a headland-bay beach—Nearshore current circulation. *Coast. Eng.* **2010**, *57*, 160–175. [CrossRef]
55. Kirby, J.T.; Dalrymple, R.A. A parabolic equation for the combined refraction–diffraction of Stokes waves by mildly varying topography. *J. Fluid Mech.* **1983**, *136*, 453. [CrossRef]
56. Battalio, B.; Chandrasekera, C.; Divoky, D.; Hatheway, D.; Hull, T.; O'Reilly, B.; Seymour, D.; Srinivas, R. *FEMA Coastal Flood Hazard Analysis and Mapping Guidelines—Wave Transformation*; Focused Study Report; Federal Emergency Management Agency (FEMA): Washington, DC, USA, 2005.
57. Secretaría de Marina. *Catálogo de Cartas y Publicaciones Náuticas 2022*; Secretaría de Marina: Mexico City, Mexico, 2022.
58. Koch, E.W.; Ailstock, S.; Stevenson, J.C. Beyond light: Physical, geological and chemical habitat requirements. In *Chesapeake Bay Submerged Aquatic Vegetation Water Quality and Habitat-Based Requirements and Restoration Targets: A Second Technical Synthesis*; Environmental Protection Agency: Washington, DC, USA, 2000; pp. 71–94.
59. Madsen, J.D.; Chambers, P.A.; James, W.F.; Koch, E.W.; Westlake, D.F. The interaction between water movement, sediment dynamics and submersed macrophytes. *Hydrobiologia* **2001**, *444*, 71–84. [CrossRef]
60. Adame, M.F.; Zaldívar-Jimenez, A.; Teutli, C.; Caamal, J.P.; Andueza, M.T.; López-Adame, H.; Cano, R.; Hernández-Arana, H.A.; Torres-Lara, R.; Herrera-Silveira, J.A. Drivers of mangrove litterfall within a karstic region affected by frequent hurricanes. *Biotropica* **2013**, *45*, 147–154. [CrossRef]
61. Lowe, R.J. Spectral wave dissipation over a barrier reef. *J. Geophys. Res.* **2005**, *110*, C04001. [CrossRef]
62. Barbier, E.B.; Hacker, S.D.; Kennedy, C.; Koch, E.W.; Stier, A.C.; Silliman, B.R. The value of estuarine and coastal ecosystem services. *Ecol. Monogr.* **2011**, *81*, 169–193. [CrossRef]

63. Koch, E.W.; Barbier, E.B.; Silliman, B.R.; Reed, D.J.; Perillo, G.M.; Hacker, S.D.; Granek, E.F.; Primavera, J.H.; Muthiga, N.; Polasky, S.; et al. Non-linearity in ecosystem services: Temporal and spatial variability in coastal protection. *Front. Ecol. Environ.* **2009**, *7*, 29–37. [[CrossRef](#)]
64. Dean, R.G. *Equilibrium Beach Profiles: US Atlantic and Gulf Coasts*; Department of Civil Engineering and College of Marine Studies, University of Delaware: Newark, NJ, USA, 1977.
65. van Tussenbroek, B.I.; Cortés, J.; Collin, R.; Fonseca, A.C.; Gayle, P.M.H.; Guzmán, H.M.; Jácome, G.E.; Juman, R.; Koltes, K.H.; Oxenford, H.A.; et al. Caribbean-wide, long-term study of seagrass beds reveals local variations, shifts in community structure and occasional collapse. *PLoS ONE* **2014**, *9*, e90600. [[CrossRef](#)]
66. Osorio-Cano, J.D.; Osorio, A.F.; Peláez-Zapata, D.S. Ecosystem management tools to study natural habitats as wave damping structures and coastal protection mechanisms. *Ecol. Eng.* **2019**, *130*, 282–295. [[CrossRef](#)]
67. Alcérreca-Huerta, J.C.; Montiel-Hernández, J.R.; Callejas-Jiménez, M.E.; Hernández-Avilés, D.A.; Anfuso, G.; Silva, R. Vulnerability of Subaerial and Submarine Landscapes: The Sand Falls in Cabo San Lucas, Mexico. *Land* **2020**, *10*, 27. [[CrossRef](#)]
68. Li, W.; Gong, P. Continuous monitoring of coastline dynamics in western Florida with a 30-year time series of Landsat imagery. *Remote Sens. Environ.* **2016**, *179*, 196–209. [[CrossRef](#)]